Contribution to the modelling of the atomization of pesticides

M. De Luca *, A. Vallet *[1] and R. Borghi **
* Cemagref, UMR ITAP, 361 rue JF Breton, 34196 Montpellier Cedex, France
** LMA-CNRS UPR 7051, 31 chemin Joseph-Aiguier 13402 Marseille cedex 20, France

Abstract
This paper reports the findings of a modelling approach to investigate the atomization of a liquid jet issued from a hollow cone agricultural nozzle in the near orifice region. The model describes the flow inside the nozzle and the spray droplet characteristics in the dispersed region. It is based on studies in the automotive field and rocket engine. Keeping the same set of constants, the results in term of liquid dispersion and Sauter mean diameter are in good agrement with experimental studies, provided that the Reynolds Stress Model is used for the turbulence.

Introduction

Agricultural pesticide spraying commonly involves ejecting a water mixture made up of active molecules and adjuvants. During this process, some of the smallest droplets do not reach the plant and contribute to the spray drift, contaminating air, water and soils. On the other hand, large or fast droplets can rebound onto the leaves and decrease also the treatment efficiency.
Experimental studies in the agricultural field are not only complex and expensive to conduct but also depend on variable external conditions (temperature, hygrometry, wind velocity and direction, ...) whereas the modelling approach can use invariable conditions. For 30 years, the United States Department of Agriculture (USDA) Forest Service has developped models to calculate the pesticide dispersion applied by aerial application above forests. In the 1990's the north american consortium of chemical registrants called Sray Drift Task Force developped with USDA Forest Service and USDA Agricultural Research Service a Lagrangian model AgDRIFT to calculate the pestide drift at time of application [6]. This model has been critized by Stoughton *et al.* [9]. The authors carried out measurements in field of drift by lidar and compared their results with those of the AgDRIFT model. Whereas the model concluded that the totality of the product was deposited in on this side distance of 400 m of the emission source, the experiments showed that drops could be found beyond 2 km of the source. Teske *et al.* answered this criticism [11] and insist indeed on the considerable importance of the initial distribution of the drop sizes [10].
Other studies on pesticide drift have been developped. P. Miller proposed a 2D model to describe the drift of sprays resulting from flat fan nozzle [8]. Droplets are assumed to form at a distance equal to the sheet coherent length and have the same velocity as the liquid sheet. Data for those two variables come from measurements using high-speed photography. The model results have been compared to experimental ones. The conclusion of the study emphasizes in particular the importance of the correct definition of sheet velocity. Moreover, hypothesis of spherical droplet may be not valid for large droplets.
Lastly, studies have been conduct using CFD codes with an Eulerian/Lagrangian approach, considering isolated drops [5], [12]. Near the exit nozzle, this hypothesis is probably wrong.
During present work, an Eulerian model was developped to assess how the sprayed liquid is atomized into droplets. One of the model advantages is to consider liquid fragments that are not necessarily spherical. Very close to the nozzle exit, there are rather ligaments than spherical droplets. Moreover, the initial conditions (velocity, diameter) of the drops are calculated by the model and not pescribed as in the Lagrangian models.

Methods

An Eulerian one phase model is adapted to agricultural nozzles. The model has been developped in the automotive and rocket engine fields [13], [2].
The two phase flow is considered as a single phase flow composed of a liquid and a gas mixture with a highly variable density $\bar{\rho}$.
The transport equation for the mean velocity does not contain any momentum exchange terms, as the mixture of liquid and gas is considered here:

$$\frac{\partial \bar{\rho}\widetilde{u}_i}{\partial t} + \frac{\partial \left(\bar{\rho}\widetilde{u}_i\widetilde{u}_j\right)}{\partial x_j} = -\frac{\partial \bar{p}}{\partial x_j}\delta_{ij} - \frac{\partial}{\partial x_j}\left(\bar{\rho}\widetilde{u_i''u_j''}\right) \quad (1)$$

The Reynolds Stress Model (RSM) has been chosen as it has greater potential to give accurate predictions for complex flows. Abandoning the isotropic eddy-viscosity hypothesis, the RSM closes the equation (1) by solving transport equations for the Reynolds Stress tensor $\bar{\rho}\widetilde{u_i''u_j''} = \bar{\rho}\widetilde{R_{ij}}$ together with an equation for the dissipation rate $\widetilde{\epsilon}$.

$$\frac{\partial \bar{\rho}\widetilde{R_{ij}}}{\partial t} + \frac{\partial\left(\bar{\rho}\widetilde{R_{ij}}\widetilde{u}_i\right)}{\partial x_i} = D_{ij} + P_{ij} + I_{ij} + \Phi_{ij} - \bar{\rho}\widetilde{\epsilon} \quad (2)$$

where D_{ij} is the turbulent diffusion, P_{ij} the stress production , Φ_{ij} the pressure strain, $\bar{\rho}\widetilde{\epsilon}$ the dissipation and I_{ij} a term due to the variable density of the

fluid. This last term has not been included yet. It is planed to include it in the future.

$$D_{ij} = -\frac{\partial}{\partial x_k}\left(\bar{\rho}\widetilde{u_i''u_j''}u_k'' + \overline{p'u_i''\delta_{jk} + p'u_j''\delta_{ik}}\right)$$

$$P_{ij} = -\bar{\rho}\widetilde{u_i''u_k''}\frac{\partial \widetilde{u}_j}{\partial x_k} - \bar{\rho}\widetilde{u_j''u_k''}\frac{\partial \widetilde{u}_i}{\partial x_k}$$

$$I_{ij} = -\overline{u_i''}\frac{\partial \bar{p}}{\partial x_j} - \overline{u_j''}\frac{\partial \bar{p}}{\partial x_i}$$

$$\Phi ij = \overline{p'\left(\frac{\partial u_i''}{\partial x_j} + \frac{\partial u_j''}{\partial x_i}\right)}$$

It can be noted that the terms linked to the variable density of the mixture I_{ij} should also appear in Φij. $\overline{u_i''}$ has an exact expression written as:

$$\overline{u_i''} = \bar{\rho}\widetilde{u_i''Y''}\left(\frac{1}{\rho_l} - \frac{1}{\rho_g}\right)$$

where $\bar{\rho}_l$ and $\bar{\rho}_g$ are the liquid and the gas density respectively.$\rho_l = 998.2\ kg/m^3$, $\rho_g = 1.2\ kg/m^3$ in our case.
The liquid dispersion is modeled using a transport equation for the mean liquid mass fraction $\widetilde{Y}$:

$$\frac{\partial \bar{\rho}\widetilde{Y}}{\partial t} + \frac{\partial\left(\bar{\rho}\widetilde{Y}\widetilde{u}_i\right)}{\partial x_i} = -\frac{\partial}{\partial x_i}\left(\bar{\rho}\widetilde{u_i''Y''}\right) \quad (3)$$

The liquid turbulent diffusion is treated using a classical gradient law:

$$\bar{\rho}\widetilde{u_i''Y''} = -\bar{\rho}\frac{\nu_t}{Sc_t}\frac{\partial \widetilde{Y}}{\partial x_i} \quad (4)$$

where Sc_t is the turbulent Schmidt number, $Sc_t = 0.7$, $\nu_t = C_\mu \widetilde{k}^2/\epsilon$, C_μ=0.09 and $\widetilde{k} = (\widetilde{u_i''u_i''})/2$.
A correction term added to the RHS of the equation (4) proposed by Demoulin [4] in the case of a co-flow was negligible in our case.
The mean density is related to the mean liquid mass fraction by:

$$\frac{1}{\bar{\rho}} = \frac{\widetilde{Y}}{\rho_l} + \frac{1-\widetilde{Y}}{\rho_g} \quad (5)$$

The mean liquid volume fraction $\overline{\tau}$ is obviously linked to $\widetilde{Y}$ by:

$$\overline{\tau} = \frac{\bar{\rho}\widetilde{Y}}{\rho_l} \quad (6)$$

The liquid dispersion was calculated using eqs. (1), (2), (3), (4), (5). In order to get the mean droplet diameter, a transport equation for the mean liquid/gas interface density $\overline{\Sigma}$ was solved. $\overline{\Sigma}$ is the quantity of the mean interfacial surface area per unit of volume, in m^{-1}. This equation is based on the transport equation for the flame density in the combustion field [7].

$$\frac{\partial \overline{\Sigma}}{\partial t} + \frac{\partial \overline{\Sigma}\widetilde{u}_i}{\partial x_i} = \frac{\partial}{\partial x_i}\left(\frac{\nu_t}{Sc_\Sigma}\frac{\partial \overline{\Sigma}}{\partial x_i}\right) + (A+a)\,\overline{\Sigma} - V_a\overline{\Sigma}^2 \quad (7)$$

$$A = -\frac{\widetilde{u_i''u_j''}}{\widetilde{k}}\frac{\partial \widetilde{u}_i}{\partial x_j}$$

$$a = a_{turb} + a_{coll}$$

$$a_{turb} = \frac{\widetilde{\epsilon}}{\widetilde{k}}, a_{coll} = \frac{C_\mu^{1/2}}{(36\pi)^{2/9}}\frac{\overline{\Sigma}^{2/3}\widetilde{\epsilon}^{1/3}}{\tau^{4/9}}$$

$$V_a = \frac{a\rho_l r_{eq}}{3\bar{\rho}\widetilde{Y}}$$

$$r_{eq} = \frac{\sigma^{3/5}(\bar{\rho}\widetilde{Y})^{2/15}}{\widetilde{\epsilon}^{2/5}\rho_l^{11/15}}$$

A represents the production of mean interfacial surface by the mean flow streching. $A = P_{ii}/\widetilde{k}$. It takes into account the mean velocity gradients and the flow anisotropy.
a_{turb} represents the production by the turbulence and is equal to the inverse of the integral time scale of turbulence.
a_{coll} is actually a collision time. It takes into account a collision length scale $L_{coll} = n^{-1/3}$ where n is the number of droplets per volume unit and a characteristic velocity $v_{coll} = (\widetilde{\epsilon}L_{coll})^{1/3}$.
The last term of the equation (7) RHS is a destruction term due to coalescence. Supposing that an equilibrium is reached between production and destruction far from the nozzle exit, $V_a = a/\overline{\Sigma}_{eq}$, with $\overline{\Sigma}_{eq} = \frac{3\bar{\rho}\widetilde{Y}}{\rho_l r_{eq}}$. r_{eq} is reached when collision and coalescence are in equilibrium. During a collision, it is supposed that all the initial kinetic energy is transformed into surface energy.
The Sauter mean diameter d_{32} can be derived from the mean liquid mass fraction equation (3) and the mean liquid/gas interface density equation (7):

$$d_{32} = \frac{6\bar{\rho}\widetilde{Y}}{\rho_l\overline{\Sigma}} \quad (8)$$

Results

The model was applied to an hollow cone nozzle particularly used in arboriculture and vineyard as fongicide and insecticide treatment. The computations are obtained on a half three dimensional grid with periodic conditions. The calculation domain, shown in Fig. 1, is composed of two parts: the nozzle itself (top of the figure) bordered by walls and the outlet domain (half of cylinder with 7.2 mm radius and 5.5 mm in heigth). A tangential canal leads the liquid into the conical swirl chamber. It exits through a hole of D=0.92 mm diameter. Due to the vortexing this causes the spray to come out in a cone shape. Boundary conditions correspond to the ones used in arboriculture : the injection pressure is fixed at 5 bar, downstream a pressure outlet condition is imposed.
The computations were performed using the CFD code Fluent version 6.2.16 [1]. The geometry was generated with the Gambit 2.2 software package. The

numerical grid constructed was consisting of 430, 000 cells. The narrower diameter of the nozzle D was composed of 20 cells.
A steady approach has been considered, so the local time derivative terms of the set of equations (1), (2), (3), (7) are neglected.
The total computational time was of the order of 12 hours on a Pentium 4 running with a 3.2 GHz processor.

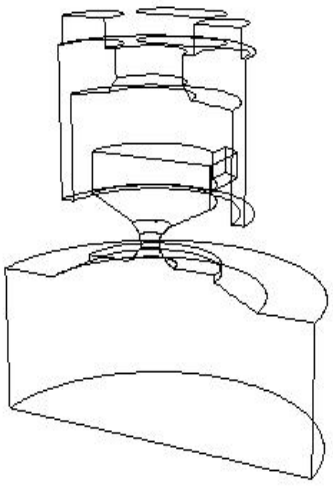

Figure 1: Computational domain

The mean liquid mass fraction $\widetilde{Y}$ is equal to 1 in the nozzle itself as it is full of water as shown in Fig. (2). Downstream one can recognise a hollow cone spray, with the smallest values of $\widetilde{Y}$ in the spray center and spray edges.

Figure 3 represents radial distribution of the mean volume fraction τ defined by the eq. (6) at 3 axial distances from the nozzle exit. Hollow cone spray spray is confirmed by the minimum value of the volume fraction at the spray axis (*i.e.* radial distance = 0), in accordance with experimental results [3]. As the distance from the nozzle increases, spray spreading in the radial direction can be observed.
Figures 3 and 4 show that inside the hollow cone liquid sheet appears a large recirculation of air flow.

Radial profiles of the mean turbulent kinetic energy are presented Fig. 5. This quantity comes from the Reynolds Stress Model, $\widetilde{k} = (\widetilde{u_i'' u_i''})/2$. It is maximum on the liquid sheet edges. The second peak at the axial position z/D=1 is not realistic. It is a numerical problem for the flow between the divergent wall edge of the nozzle and the pressure outlet edge. It should be corrected in the future.

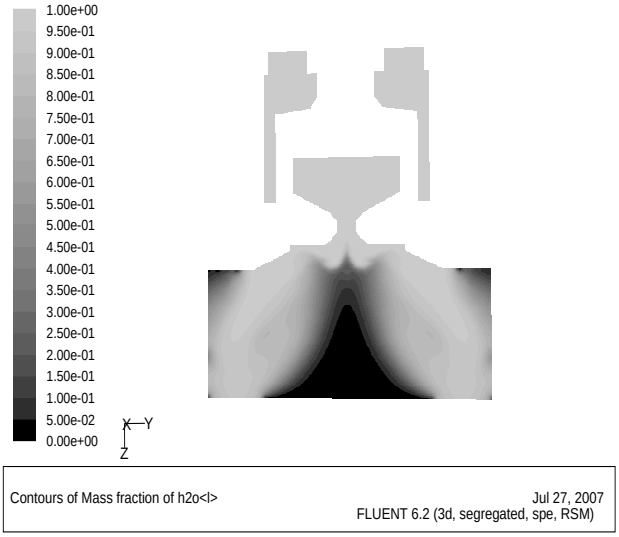

Figure 2: Contours of the mean liquid mass fraction on the periodic faces of the domain

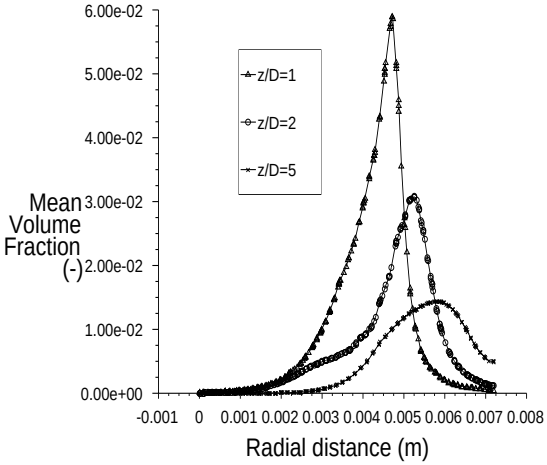

Figure 3: Radial profiles of the volume fraction for three axial positions

Radial profiles of the mean liquid/gas interface density are presented Fig. 6. They are quite similar to the profiles of the volume liquid fraction, as interface exists only if liquid exists. Nevertheless, it can be surprising that the maximum of interface density is not found on the spray edges (i.e. large gradients of the mean volume fraction), where the interface production should be maximum. The different terms of

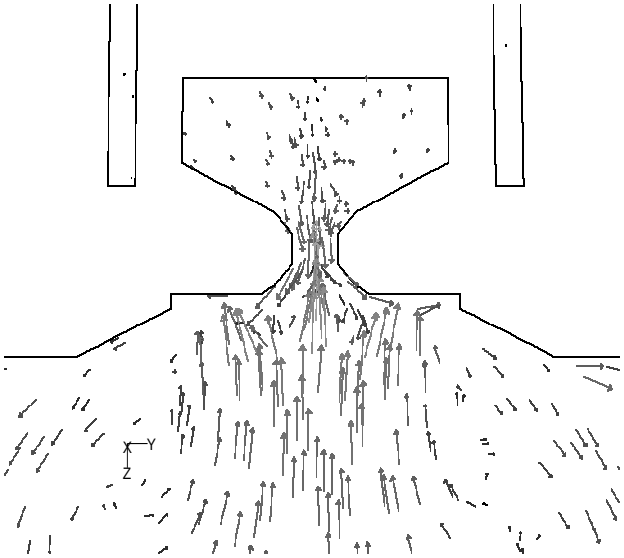

Figure 4: Velocity vectors in the swirl chamber and near the nozzle exit

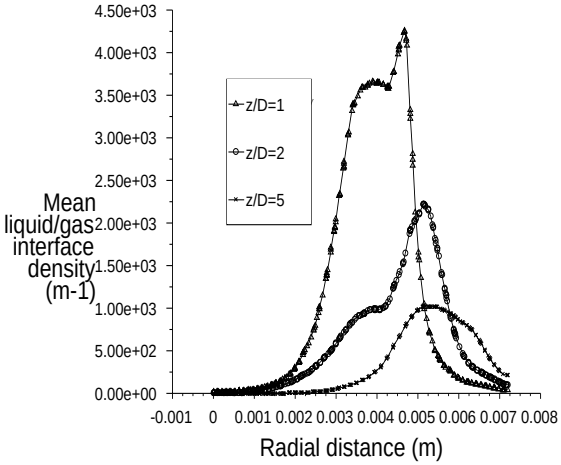

Figure 6: Radial profiles of the mean liquid/gas interface density for three axial positions

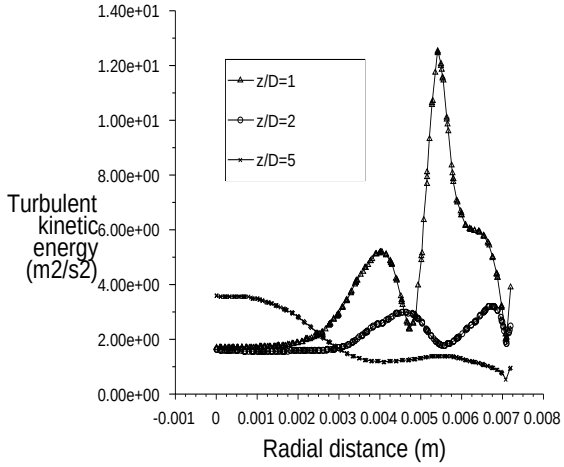

Figure 5: Radial profiles of the mean turbulent kinetic energy $\widetilde{k} = (\widetilde{u_i'' u_i''})/2$ for three axial positions

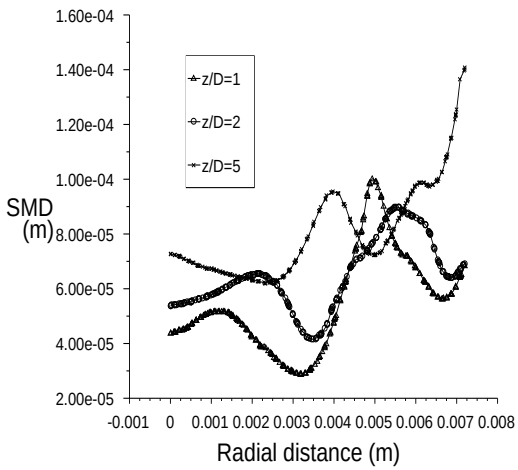

Figure 7: Radial profiles of the Sauter Mean Diameter for three axial positions

the $\overline{\Sigma}$ should be more examinated.

The Figure 7 presents the radial distribution of the Sauter mean diameter calculated from the equations for the mean liquid mass fraction and the mean interface density (see eq. (8)).
An experimental study involving an optic sensor is in progress. A mean presence liquid rate and a mean velocity in the dense region of the spray are measured. The magnitude orders of the Sauter Mean Diameter calculated through the model are in good agreement with experimental preliminary results.
Largest SMD on the spray edges could be linked to coalescence as the turbulent kinetic energy is law. Nevertheless, in this region, there is only little liquid. In other words, these big droplet appear only rarely.

Conclusions and perspectives

The predictive capability of the Eulerian atomisation model has been demonstrated for a agricultural hollow cone nozzle. The constants included in the model have been chosen equal to those taken by authors in automotive and rocket engine fields. The liquid dispersion is in good agreement with experimental results: mean liquid fraction profiles confirm the presence of a hollow cone spray. Moreover, the SMD values are in the same magnitude order as the ones given by the experience. Experimental results are still in progress.
The short term perspective will be to examine the study concerning the variable density term in the equations.
The long term perspective will concern the coupling between this Eulerian model with a Lagrangian approach to describe the entire trajectory of pesticide droplets.

Acknowledgements

Magali De Luca was supported by a joint grant from Cemagref and ADEME (French Environment and Energy Management Agency).

Nomenclature

d_{32}	Sauter Mean Diameter	m
$\widetilde{k}$	turbulent kinetic energy	m^2/s^2
$\bar{p}$	mean pressure	Pa
R_{ij}	Reynolds Stress tensor	m^2/s^2
$\widetilde{u_i}$	mean velocity	m/s
u"	fluctuating velocity	m/s
$\widetilde{Y}$	mean liquid mass fraction	-
$\widetilde{Y''}$	fluctuating liquid mass fraction	-
$\widetilde{\epsilon}$	turbulent dissipation rate	m^2/s^3
$\bar{\rho}$	mean density	kg/m^3
σ	surface tension coefficient	N/m
$\overline{\Sigma}$	mean interfacial density	m^{-1}
τ	mean volume liquid fraction	-

References

[1] Fluent 6-1 User's Guide. Technical report, Fluent Inc., 2003.

[2] Beau P.A., Lebas R., Funk M., Demoulin F.X. Multiphase Flow approach and single phase flow approach in the context of euler model for primary break up. In *19th ILASS*, Nottingham, 2004.

[3] Ben L., Vallet A., Bonicelli B. Atomisation of agricultural sprays: influence of some liquid properties. In *19th ILASS*, Nottingham, 2004.

[4] Blokkeel G., Mura A., Demoulin F.X. and Borghi R. A continous modeling approach for describing the atomization process from inside the injector to the final spray. In *ICLASS*, Sorrento, 2003.

[5] Brown, R., Sidahmed, M.M. Simulation of spray dispersal and deposition from a forestry airblast sprayer - Part II : Droplet trajectory model. *Transactions of the ASAE*, Vol. 44(1):pp. 11–17, 2001.

[6] Hewitt A.J., H.W. Thistle and M.E. Teske. AgDRIFT: Applied Modeling Tool for Aerial Spraying. In *Annual Gypsy Moth Review*, Norfolk VA., 2000.

[7] Marble F.E and Broadwell J.E. The coherent flame model for turbulent chemical reactions. Tech report trw-9-pv, Project Squid Headquarters - Chaffee Hall - Purdue University, 1977.

[8] Miller, P.C.H. and Hadfield D.J. A simulation model of the spray drift from hydraulic nozzles. *J. agric. Engng Res.*, Vol. 42:pp. 135–147, 1989.

[9] Stoughton, T.E., Miller, D.R., Yang, X., Ducharme, K.M. A comparison of spray drift predictions to lidar data. *Agricultural and Forest Meteorology*, Vol. 88:pp. 15–26, 1997.

[10] Teske, M.E., Barry, J.W. Parametric sensitivity in aerial application. *Transactions of ASAE*, Vol. 36(1):pp. 27–33, 1993.

[11] Teske, M.E., Thistle, H.W. Comments on "A comparison of spray drift predictions to lidar data" by T.E Stoughton, D.R. Miller, X. Yang, K.M.Ducharme. *Agricultural and Forest Meteorology*, Vol. 93:pp. 283–285, 1999.

[12] Tsay, J., Fox, R.D., Ozkan, H. E., Brazee, R.D., Derksen, R.C.,. Evaluation of a pneumatic-shielded spraying system by CFD simulation,. *Transactions of ASAE*, 45(1):47–54, 2002.

[13] Vallet A., Burluka A.A., Borghi R. Development of an eulerian model for the atomisation of a liquid jet. *Atomization and Sprays*, Vol. 11(6):pp. 619–642, 2001.